

Critical fluctuations in the weak itinerant ferromagnet Ni₃Al: A comparison between self-consistent renormalization and mode-mode coupling theory

F. Semadeni, B. Roessli, and P. Böni

Laboratorium für Neutronenstreuung ETH-Zürich & PSI, CH-5232 Villigen PSI, Switzerland

P. Vorderwisch

Hahn-Meitner Institut, D-14109 Berlin, Germany

T. Chatterji

Institut Laue Langevin, BP 156, 38042 Grenoble Cedex 9, France

(Received 9 February 2000)

The magnetic excitations in the weak itinerant ferromagnet Ni₃Al have been investigated in the ordered phase as well as in the paramagnetic phase by means of inelastic neutron scattering, in order to search for critical fluctuations. The magnetic excitations have been interpreted within the framework of both itinerant and mode-mode coupling theory (MMT) for an isotropic ferromagnet. The parametrization of the linewidth for the critical scattering shows that the dynamical critical exponent $z \approx 2.47 \pm 0.16$ is close to the value expected for an isotropic Heisenberg model, proving that critical fluctuations are also important in weak-itinerant ferromagnets. Moreover, the temperature dependence of the spin waves compares well with the predictions of MMT. The correlation length in weak itinerant magnets is very large leading to pronounced short-range order and to critical fluctuations far away from T_C . The results show that it is necessary to include critical fluctuations in the theory for itinerant magnetism.

I. INTRODUCTION

Magnetic excitations in weak itinerant ferromagnets are interesting model systems for the investigation of strongly correlated materials that have attracted recently significant attention because of the discovery of high-temperature superconductivity and the renewed interest in the metal-insulator transition in oxide transition-metal materials, for example, in doped LaMnO₃.

Weak itinerant ferromagnets are characterized by a low Curie temperature T_C when compared with the energy scale of the magnetic fluctuations and a small magnetic moment, the reason being that the conduction electrons are mainly responsible for the magnetic properties of these compounds. A model to calculate T_C was proposed by Stoner¹ who considered a single-band system. This model can explain the T dependence of the magnetization at low T , however, the calculated T_C 's are typically one order of magnitude too high because the gain in energy arising from spin fluctuations is neglected. Long-range order is lost due to the vanishing amplitude of the magnetic moments at T_C . This behavior is in marked contrast to a localized ferromagnet, where long-range order is destroyed by the thermal excitation of spin waves.

In order to resolve these problems, Moriya² and Lonzarich³ pointed out the importance of low-energy spin fluctuations in itinerant magnets and used self-consistent renormalization theory (SCR) and a phenomenological magnetic equation of state within the random-phase approximation (RPA), respectively, in order to take into account the thermodynamic properties of fluctuations. These theories are able to predict values for T_C and for the ratio p_{eff}/p_0 of the

moments above and below T_C that are in good agreement with experiments on MnSi and Ni₃Al. In addition, the predicted quadratic q dependence of the spin-wave dispersion has been confirmed in experiments.⁴⁻⁶

Most interestingly, however, is the prediction that the q dependence of the linewidth of the magnetic fluctuations is markedly different when compared with a localized ferromagnet, i.e.,

$$\Gamma_{wi} = A_{wi} q [q^2 + (\kappa^\pm)^2] \quad (1)$$

versus

$$\Gamma_{loc} = A_{loc} f_\Gamma(\kappa^\pm/q) q^{2.5}. \quad (2)$$

The former expression has been confirmed for $T \geq T_C$ by Ishikawa, Shirane, and Tarvin in weak itinerant MnSi that exhibits below T_C a helical structure.⁴ More recent experiments on polycrystalline Ni₃Al by Bernhoeft and co-workers^{5,6} also indicate the validity of Γ_{wi} .

On the other hand, the inspection of spin dynamics near the ordering temperature leads to consider scaling relations. For a Heisenberg magnet, the dynamical scaling function $f_\Gamma(\kappa^\pm/q)$ is equal to 1 at T_C and is a homogeneous function of κ^\pm/q away from T_C . According to static scaling theory, the inverse of the spin correlation length is given by $\kappa^\pm = \kappa_0^\pm (|T - T_C|/T_C)^{0.702}$, where \pm refers to measurements above and below T_C , respectively.

The nonexistence of critical fluctuations in weak-itinerant magnets seems to be surprising due to the following reason: In contrast to a localized magnet, where the magnetic moments are confined to single atoms, the magnetic moments in itinerant magnets are defined over large assemblies of atoms that are correlated over a distance $\xi_c \gg a$, where a is the

lattice parameter. As soon as the correlation length of the magnetic fluctuations ξ^\pm and the wavelength of the spin fluctuations $\Lambda = 2\pi/q$ exceed ξ_c one may argue that one should observe critical fluctuations similarly as in true local moment systems.

In order to test the existence of critical fluctuations we have determined the q dependence of the quasielastic fluctuations at T_C . We have determined the temperature dependence of the linewidth of the spin waves below T_C and compared them with the predictions of a very recent mode-mode coupling theory.⁷⁻⁹ We have also studied the temperature dependence of the paramagnetic excitations, which was found to be in agreement with the scaling function predicted for itinerant systems above T_C .³ The results show that Ni_3Al is one of the most ideal and clean systems to prove the dynamical scaling behavior in an isotropic ferromagnet below T_C .

II. EXPERIMENTAL PROCEDURE

The inelastic neutron-scattering experiments have been performed on a cylindrical Ni_3Al single crystal with a diameter of 16 mm and a length of 60 mm, enriched with Ni. The enrichment by 1% Ni has no influence on the fcc structure of the sample, however, it leads to an enhancement of the magnetic moment and to a larger T_C thus facilitating the experiment. Magnetization measurements performed on pieces taken from the top and the bottom of the single crystal yielded consistent values $T_c = 72.5 \pm 0.5$ K in excellent agreement with values reported in Ref. 10 for a sample with 1% enrichment. More evidence for the high quality of the sample will be given below.

The experiments have been carried out on the cold neutron three-axis spectrometers FLEX at the HMI in Berlin, and TASP at the Swiss spallation source SINQ. The same experimental setup has been used for both experiments. The final energy was fixed at $E_f = 2.5, 3.0,$ and 4.5 meV and tight collimations (guide-20'-20'-40') were used, leading to a resolution of 0.03, 0.04, and 0.09 meV, respectively. A cold Be filter was placed in the incident beam to remove higher-order neutrons. The background was measured at $T = 1.5$ K for all configurations and subtracted from the data. As in this work we were primarily interested in spin-wave excitations, the forward scattering technique was chosen for convenience, thus avoiding phonon contributions.

The data have been fitted with a double Lorentzian scattering function for damped spin waves:

$$S(q, E) = \frac{E}{1 - e^{-\beta E}} \frac{N}{q^2} \frac{1}{2\pi} \left[\frac{\Gamma}{(E + E_q)^2 + \Gamma^2} + \frac{\Gamma}{(E - E_q)^2 + \Gamma^2} \right], \quad (3)$$

and the deconvolution with respect to the resolution of the spectrometer was performed. In Eq. (3) N is a normalization constant, $E_q = D(T)q^2$ is the dispersion, and Γ is the relaxation frequency (linewidth) of the magnetic excitations. The quantity N/q^2 is proportional to the static susceptibility $\chi_\perp(q)$. To fit the data at T_C , the spin-wave energy E_q was set to zero.

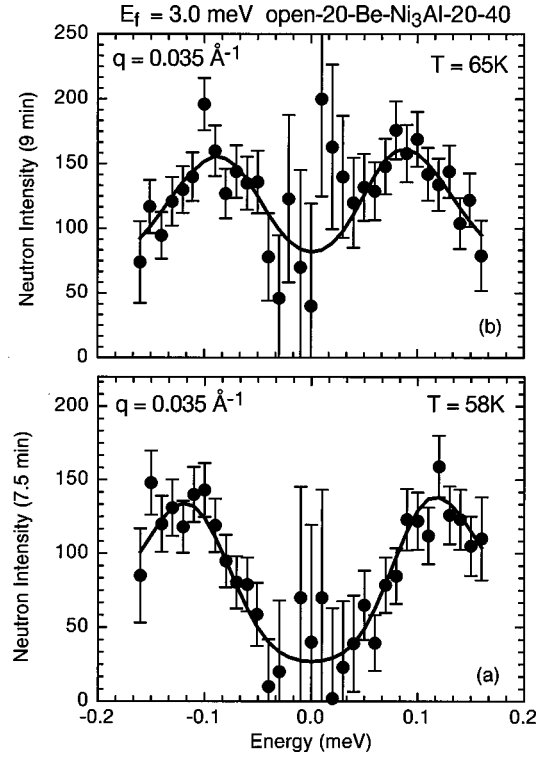


FIG. 1. Inelastic scans at $q = 0.035 \text{ \AA}^{-1}$ for $T = 0.8$ and $0.9 T_C$. The solid lines are fits to the model given by Eq. (3) convoluted with the experimental resolution function.

We have used an iterative process to obtain the parameters N , D , and Γ from the inelastic scans. In a first step all parameters were free. In a second step we fixed D for each T at an averaged value. Finally, the linewidth was fixed too and N was determined. This procedure reduced correlation effects between E_q , $\Gamma(q)$, and $\chi_\perp(0)$ considerably.

In order to determine which model best describes the collective excitations in Ni_3Al , we have systematically analyzed the data using itinerant³ and localized theory,^{8,9} respectively, i.e., we assumed that the q dependence of Γ is given by Eqs. (1) and (2), respectively.

III. RESULTS

Some typical results of inelastic scans after subtraction of the background measured at $T = 1.5$ K are shown in Fig. 1. The error bars around $E = 0$ meV are large due to the important incoherent scattering of Ni. The renormalization of the spin waves with increasing temperature is clearly visible. The tails of the spectra cannot be measured because the scattering triangle does not close at high-energy transfers anymore.

For each T the measured spin-wave dispersion was fitted with the quadratic expression $E_q = \Delta + Dq^2$. The fits show that the energy gap Δ is vanishingly small at all T . The T dependence of D is plotted in Fig. 2 and shows clearly the renormalization of the spin waves close to T_C .

According to the itinerant model, the spin waves are expected to occur at finite-energy transfer with a dispersion proportional to the magnetization M :

$$E_q = g\mu_B M \chi_\perp^{-1}(q) = g\mu_B M (\chi_\perp^{-1} + c_\perp q^2 + \dots). \quad (4)$$

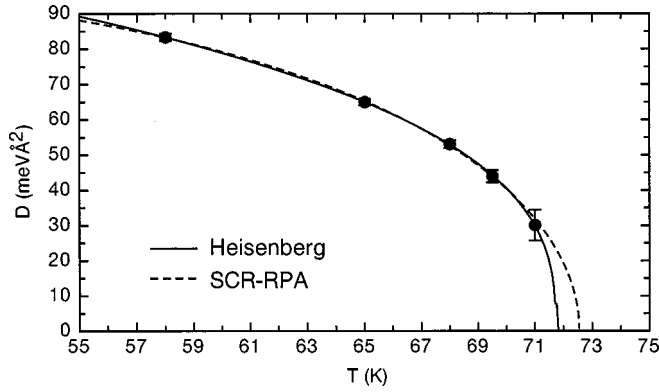


FIG. 2. Spin-wave stiffness as a function of temperature, the solid line is related to the Heisenberg model, and the dashed line to the itinerant model.

The spectroscopic splitting factor g is close to 2 in Ni_3Al . M is predicted to behave according to

$$M(T,0)/M_0 = [1 - (T/T_c)^\epsilon]^{1/2}, \quad (5)$$

where ϵ is equal to 2 in the Stoner model and $4/3$ in the SCR theory.³

In contrast, the spin-wave dispersion for a Heisenberg ferromagnet is given for $T \rightarrow T_c$ by

$$E_q = D(T)q^2 = D_0|\tau|^{0.36}q^2, \quad (6)$$

where $\tau = 1 - T/T_c$.

The temperature dependence of the spin-wave stiffness D has been fitted using the itinerant [see Eq. (5)] and the localized model [see Eq. (6)]. If the ordering temperature is fixed at $T_c = 72.5$ K, as obtained from the magnetization measurements, the exponent ϵ of the itinerant model differs from the $\epsilon = 4/3$ value (see dashed curve in Fig. 2). On the contrary, fixing ϵ at the predicted value gives a slightly higher value for the transition temperature (74 ± 0.4 K). This discrepancy between the experimental and the theoretical T_c is of the same order of the one observed for polycrystalline samples.¹¹ On the other hand, the fit with the Heisenberg model gives an exponent of 0.34 ± 0.03 , close to the theoretically expected $0.36(5)$ value, and is much less sensitive to T_c (solid curve in Fig. 2). As a comparison, the ratio of $D(0.8T_c)$ for our sample and D_p for the polycrystalline reference of pure Ni_3Al ⁶ gives $D/D_p = 1.38 \pm 0.08$, a value that shows reasonable agreement with the ratio of the magnetic moments measured in both kind of samples¹⁰ ($D/D_p = 1.65$).

In Eq. (4) $\chi_\perp = \chi_\perp(q=0)$ is the static transverse susceptibility that is infinity if there is no anisotropy. Our results show that $\chi_\perp(q=0) = \infty$ within the accuracy of the neutron measurements. This behavior is actually expected, since the spin waves are Goldstone modes, irrespective of the degree of localization of the spins.

The static susceptibility $\chi_\perp(q)$ resulting from the integration of the inelastic signal over energy was extracted from the data. Figure 3 shows $\chi_\perp^{-1}(q)$ versus q^2 . The linear relationship is in agreement with the expected $1/q^2$ divergence for spin waves. Within the experimental accuracy the inverse correlation length for the spin waves $\kappa_\perp = 0.016 \pm 0.017 \text{ \AA}^{-1}$ (not to be confused with κ_0^-) is zero, in agree-

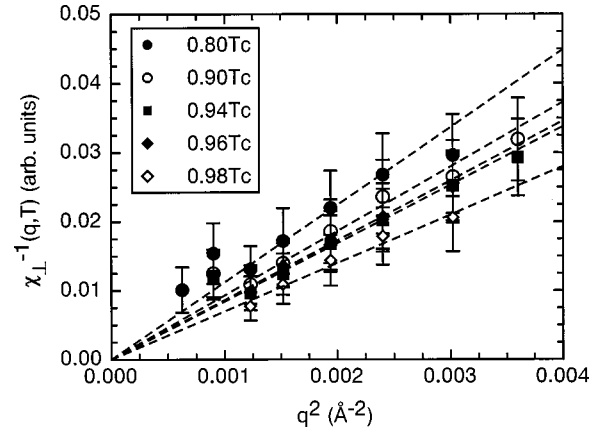


FIG. 3. The inverse of the static susceptibility of the spin waves, $\chi_\perp^{-1}(q)$, as a function of q^2 , the dashed lines are fits to the data using a Lorentzian q dependence: $\chi(q)_\perp^{-1} \propto (\kappa_\perp^2 + q^2)$. The parameter κ_\perp was found to be zero within the accuracy of the measurements.

ment with the observation that the spin waves have no gap. In addition, the slope of $\chi_\perp(q)$ shows a slight T dependence, which is connected to the fact that $\chi(T)_{q=0}$ increases by approaching T_c .

The linewidth of the spin waves is plotted in Fig. 4 and compared with SCR theory (a) (fit parameters A_{wi} and κ^-) and scaling theory based on the Heisenberg model (b) (fit parameters A_{loc} and z). The comparison shows that both

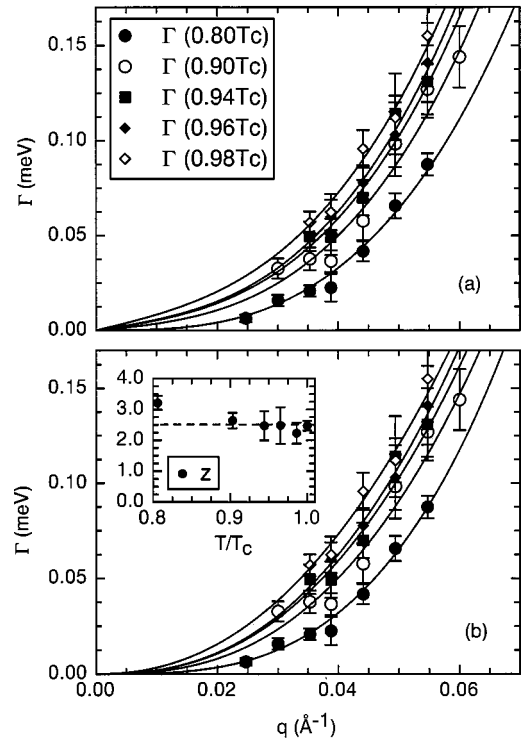


FIG. 4. Resolution corrected spin-wave linewidth $\Gamma(q)$, plotted as a function of q , for several temperatures. The plot (a) shows a fit with the itinerant model, whereas in (b), a fit with the Heisenberg model has been used. The inset displays the experimental critical exponent z as a function of temperature. The exponents are close to the 2.5 Heisenberg value (dashed line).

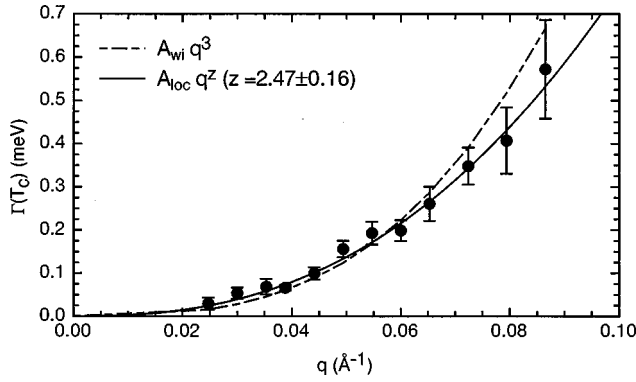


FIG. 5. Quasielastic linewidth measured at T_C . The solid line is a fit to the Aq^z model, whereas for the dashed line the exponent has been fixed at 3, as expected from itinerant theory.

models provide good parametrizations of the data. The inset shows that the critical exponent z is close to the value 2.5 that has been predicted theoretically and measured in many ferromagnetic systems (see Ref. 9 for a summary). We point out that this behavior occurs over a large T range.

In order to provide a direct comparison of the spin fluctuations in Ni_3Al with scaling theory we have measured the linewidth of the paramagnetic fluctuations at T_C (see Fig. 5). The solid line is a fit to the data using the expression $\Gamma = Aq^z$ yielding $z = 2.47 \pm 0.16$ that is compatible with the dynamical scaling prediction $z = 2.5$ at $T = T_C$. In contrast, the RPA expression $\Gamma = A_{wi}q^3$ does not reproduce the data well.

In a second step we divided for each temperature the resolution corrected linewidth $\Gamma(T)$ by $\Gamma(T = T_C)$ (measured values) in order to determine $f_\Gamma(\kappa^-/q)$ [see Eq. (2)]. The scaling function is plotted in Fig. 6 versus the scaling variable $x = \kappa^-/q$. As the inverse correlation length κ^- is not known below T_C we have adjusted the scale of the x axis such that the data points agree with the theoretical curve of mode-mode coupling theory (MMT) of Ref. 8. The comparison yields $\kappa_0^- = 0.10 \pm 0.04 \text{ \AA}^{-1}$.

Finally, we have analyzed the scaling behavior of the magnetic excitations above T_C , as shown in Fig. 7. The scaling variable $x = \kappa^+/q$ has been determined as follows. According to scaling laws from mode-coupling theory in the

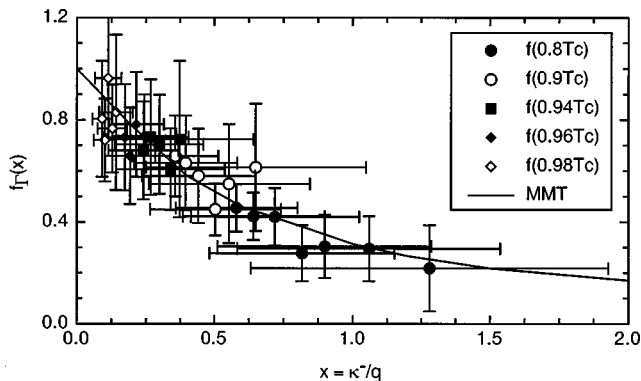


FIG. 6. Dynamical scaling function for the linewidth of the spin waves as a function of the scaling parameter $x = \kappa^-/q$. The solid line is given by mode-mode coupling theory for an isotropic ferromagnet (Ref. 8).

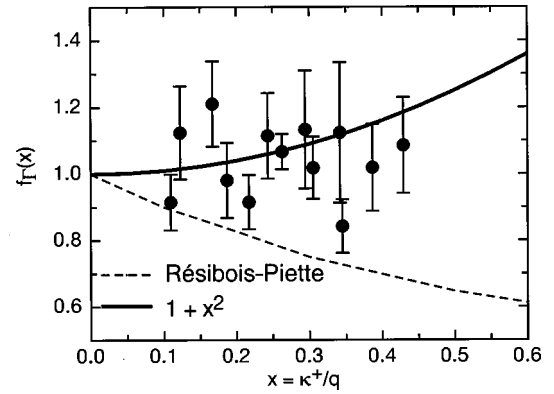


FIG. 7. Dynamical scaling function for the paramagnetic fluctuations, as a function of the scaling parameter $x = \kappa^+/q$. The dashed line represents the Résibois-Piette scaling function (Ref. 12), whereas the solid line ($1 + x^2$) is provided by SCR (Ref. 2).

critical regime, the ratio for the inverse correlation length below and above T_C is given by $\kappa^-/\kappa^+ = 2.02$. We have therefore used the experimental value κ_0^- determined with the scaling of the spin waves, that yielded $\kappa_0^+ = 0.049 \pm 0.019 \text{ \AA}^{-1}$. Since the paramagnetic signal has to be recovered by background subtraction from the top of a large incoherent signal, more experimental time is required for obtaining the same statistics as in the ordered phase, where the magnetic excitations are dispersive. Therefore we could not gather so many datapoints as for the ferromagnetic case in a reasonable time. Nevertheless, the experimental scaling function above T_C provides sufficient information for allowing us to compare it with theoretical predictions. We have plotted in Fig. 7. the Résibois-Piette function,¹² which results from MMT calculations for a Heisenberg system, as well as the “ $1 + x^2$ ” scaling law from SCR theory.² In the case of paramagnetic scattering, we observe that Ni_3Al shows better agreement with the predictions of the theory for itinerant systems.

IV. DISCUSSION

The analysis of the magnetization and the q dependence of the spin waves does not allow an unambiguous distinction between MMT and SCR. In order to obtain a more detailed comparison, we have inspected the scaling behavior of the linewidth of the spin waves, $f_\Gamma(x)$, near T_C , in the light of MMT that includes critical fluctuations and dipolar interactions (see Fig. 6). As the magnetic moments in Ni_3Al are small, we considered the special case of the isotropic limit.⁸

It is seen that below T_C the data as well as MMT yield a monotonic decrease of $\Gamma(q, T)$ with decreasing T . This behavior is in contradiction to the RPA result that predicts an increase of $\Gamma(q, T)$ with decreasing T (Ref. 3). We argue that the q range probed by the experiment corresponds to wavelengths of spin waves Λ that are much larger than the correlation distance ξ_c that defines the magnetic moments. Therefore the moments can be considered to be localized with respect to the spin excitations thus masking itinerant effects.

The universality of the spin-wave frequency for ferromagnets has been highlighted by Schinz and Schwabl⁹ within the framework of MMT. In the critical regime, the scaling am-

plitude W_- connects the spin-wave frequency and the damping at T_C :

$$W_- = \frac{D_0}{A\sqrt{\kappa_0^-}}, \quad (7)$$

where D_0 is the spin-wave stiffness at $T=0$, A is related to the spin-wave linewidth at T_C , $\Gamma(T_C)$, and κ_0^- refers to the inverse correlation length. For Ni_3Al , we obtain $W_- = 1.88 \pm 0.56$. This value lies within the range of the parameters for other ferromagnets like Fe, Ni, Co, EuO, and EuS, where $1.24(14) \leq W_- \leq 2.07(9)$ (see Ref. 9). Moreover, inelastic neutron-scattering experiments performed in these ferromagnets have shown that $\Gamma(T_C)$ can be well parametrized by $Aq^{2.5}$, leading to the conclusion that the spin dynamics in localized and weak itinerant ferromagnets show a universal behavior at T_C .

The q dependence of the linewidth at T_C and the experimental scaling function below T_C indicate that the critical scattering cannot be neglected for describing the spin dynamics of Ni_3Al in the ordered phase.

Above T_C the interpretation of the results is less clear. Our results from single-crystal Ni_3Al agree well with previous results obtained from polycrystalline Ni_3Al .^{5,11} In fact, $\Gamma(q, T)$ shows a similar behavior as in other well-known itinerant systems like MnSi (Ref. 13) and CoS_2 (Ref. 14) and the results seem to be in agreement with predictions of SCR and RPA theory, i.e., $\Gamma(q)$ in the paramagnetic phase is given by Eq. (1).

The question arises why we observe dynamical scaling behavior below T_C on the one hand and ‘‘itinerant’’ behavior above T_C on the other hand. We interpret the discrepancy between the scaling functions in Fig. 7 to be caused by the additional damping of the spin fluctuations by the conduction electrons. In weak itinerant ferromagnets, the mean-square local amplitude of the magnetic moments $\langle S_L^2 \rangle$ is known to be temperature dependent.² The variations are particularly important in the paramagnetic phase where $\langle S_L^2 \rangle$ increases linearly with T . The associated damping compensates for the initial decrease of the Réibois-Piette function at small x . Similar deviations from MMT have been observed in the metallic Heisenberg ferromagnet Pd_2MnSn and interpreted in terms of damping by the conduction electrons that provide the Ruderman-Kittel-Kasuya-Yosida interaction between the local moments.¹⁵ As a second example we mention Ni, where $\Gamma(T_C) = Aq^{2.5}$ (see Ref. 16) although its scaling behavior above T_C disagrees with mode-mode coupling theory.¹⁷

In the light of the above discussion on the dynamical scaling function $f_\Gamma(x)$, we cannot exclude that damping effects

also affect the spin dynamics below T_C . However, in contrast to $T > T_C$, one may argue that the combined effects of conduction electrons and critical scattering can lead to a scaling function that starts with a negative slope, if one assumes that the additional damping caused by the spin-flip excitations in the conduction band is reduced with decreasing temperature. Therefore the latter effects merely lead to a re-scaling of the scaling variable x in $f_\Gamma(x)$. The distinction between different contributions can be done by determining the inverse correlation length below T_C , κ^- . In order to access this information, it is necessary to study the longitudinal spin fluctuations using polarized neutrons.

V. CONCLUSION

The spin dynamics of weak itinerant Ni_3Al has been studied in detail by means of inelastic neutron scattering below and above the Curie temperature T_C . The experimental data was interpreted within the framework of both itinerant (SCR-RPA) and mode-mode coupling (MMT) theories for an isotropic ferromagnet. We have determined experimentally the dynamical scaling function of the magnetic fluctuations in the ordered phase as well as in the paramagnetic phase. The temperature dependence of the damping of the magnetic fluctuations could be satisfactorily explained in the ferromagnetic phase as well as at T_C by MMT. On the other hand, the scaling behavior above T_C matches with the theoretical predictions for an itinerant spin system.

According to the observed q dependence of the damping at T_C , we were tempted to analyze the dynamical scaling behavior of the spin fluctuations in the light of MMT that includes critical scattering. Nevertheless, this latter model does not take into account the itinerant character of Ni_3Al , namely the fact that the mean-square local amplitude of the magnetic moments $\langle S_L^2 \rangle$ is not constant. This feature leads to a modification of the mode-mode coupling dynamical scaling functions. The additional damping caused by the conduction electrons requires corrections for $f_\Gamma(x)$ in both magnetic phases that are qualitatively consistent with the overall behavior of our experimental curves.

On the basis of the results obtained with Ni_3Al , we propose that it would be of interest to include critical fluctuations in the magnetic equation of state of SCR, in order to explain the dynamical scaling behavior observed in weak itinerant magnets, within the framework of an itinerant model.

ACKNOWLEDGMENT

One of the authors (F.S.) would like to thank the ETH-Rat for financial support.

¹E. C. Stoner, Proc. R. Soc. London, Ser. A **165**, 372 (1938).

²T. Moriya, *Spin Fluctuations in Itinerant Electron Magnetism* (Springer, Berlin, 1985); and references therein.

³G. G. Lonzarich and L. Taillefer, J. Phys. C **18**, 4339 (1985).

⁴Y. Ishikawa, G. Shirane, and J. A. Tarvin, Phys. Rev. B **16**, 4956 (1977).

⁵N. R. Bernhoeft, G. G. Lonzarich, P. W. Mitchell, and D. McK.

Paul, Phys. Rev. B **18**, 422 (1983).

⁶N. R. Bernhoeft, G. G. Lonzarich, D. McK. Paul, and P. W. Mitchell, Physica B **136**, 443 (1986).

⁷E. Frey and F. Schwabl, Z. Phys. B: Condens. Matter **71**, 355 (1988).

⁸H. Schinz and F. Schwabl, Phys. Rev. B **57**, 8438 (1998).

⁹H. Schinz and F. Schwabl, Phys. Rev. B **57**, 8456 (1998).

- ¹⁰ F. R. de Boer, C. J. Schinkel, J. Biesterbos, and S. Proost, *J. Appl. Phys.* **40**, 1049 (1969).
- ¹¹ G. G. Lonzarich, *J. Magn. Magn. Mater.* **54**, 612 (1986).
- ¹² P. Résibois and C. Piette, *Phys. Rev. Lett.* **24**, 514 (1970).
- ¹³ Y. Ishikawa, Y. Noda, C. Fincher, and G. Shirane, *Phys. Rev. B* **31**, 5884 (1985).
- ¹⁴ H. Hiraka, Y. Endoh, and K. Yamada, *J. Phys. Soc. Jpn.* **66**, 818 (1997).
- ¹⁵ M. Kohgi, Y. Endoh, Y. Ishikawa, H. Yoshizawa, and G. Shirane, *Phys. Rev. B* **34**, 1762 (1986).
- ¹⁶ P. Böni, J. L. Martinez, and J. M. Tranquada, *Phys. Rev. B* **43**, 575 (1991).
- ¹⁷ P. Böni, H. A. Mook, J. L. Martinez, and G. Shirane, *Phys. Rev. B* **47**, 3171 (1993).